Magnetic anisotropy and temperature dependence of the hyperfine fields of ^{111}Cd in single-crystalline cobalt

N. P. Barradas
Centro de Física Nuclear da Universidade de Lisboa, Avenida Professor Gama Pinto No. 2, P-1699 Lisboa, Portugal

M. Rots
Insitut voor Kern-en Stralingsfysika, Katholieke Universiteit Leuven, Celestijnenlaan 200D, B-3001 Leuven, Belgium

A. A. Melo and J. C. Soares
Centro de Física Nuclear da Universidade de Lisboa, Avenida Professor Gama Pinto No. 2, P-1699 Lisboa, Portugal
(Received 24 August 1992)

The magnetic anisotropy of single-crystalline cobalt and the temperature dependence of the hyperfine fields of cadmium in cobalt were studied by the perturbed-angular-correlation technique without any applied magnetic field. A uniaxial basal-plane anisotropy was found instead of the expected threefold one, and was explained by lattice-deformation-induced anisotropy. The obtained temperature dependence of the angle between the magnetization and the c axis is in agreement with the uniaxial anisotropy constants K_1 and K_2 found by torque magnetometry. The room-temperature values of the hyperfine fields are $B_{hf}=288(3)$ kG and $V_{ZZ}=32(5)\times10^{15}$ V/cm^2.

I. INTRODUCTION

While the easy magnetization direction in bulk cobalt is along the c axis at room temperature, it slowly turns to the basal plane at higher temperatures. Different measurements of the magnetocrystalline anisotropy of hcp cobalt have been reported, yielding a spread of values for the uniaxial anisotropy constants K_1 and K_2 (Paige, Szpunar, and Tanner[1] and references therein). Paige, Szpunar, and Tanner proposed to take their data set together with the data of Ono[2] and Sucksmith and Thompson,[3] for an adequate analysis of the experimental data including corrections for the misalignment of the magnetization with the applied field, which improved the accuracy. The motivation of the present experiments is twofold. Ono showed that K_1 and K_2 depend on the intensity of the applied field. Therefore, an experiment to measure the magnetic anisotropy of cobalt without applying an external field can be valuable. Furthermore, the anisotropy constant K_4 corresponding to the basal plane (b plane) was also measured by Paige and co-workers. Using a single crystal cut along the b plane, they observed a threefold symmetry axis, the magnetization being in three different but equivalent directions at high temperatures. However, they couldn't determine the b-plane anisotropy for crystals cut along a plane including the c axis (c plane). The study of such crystals by a different method is undertaken in the present work.

The perturbed-angular-correlation (PAC) technique measures the hyperfine interaction between the nuclear moments of a probe nucleus and the internal fields of its environment, without need to apply an external field. The temperature dependence of the hyperfine interaction of several probe nuclei in hcp cobalt have been previously measured,[4–18] but in most cases the authors determined the value of the magnetic hyperfine field but not its direction. Lindgren, Bedi, and Wappling[18] already determined the temperature dependence of the angle between the magnetization and the c axis, using ^{111}Cd as probe nucleus. However, the agreement with the results of Sucksmith and Thompson[13] is poor, mainly because of a large uncertainty in the angle determination due to the use of a polycrystalline sample used in the former study.

For a cobalt single crystal cut along the c plane and the same ^{111}Cd probe nucleus, we determine with high precision both the magnitude and the direction of the internal magnetic field. In contrast with the use of polycrystals, here no ambiguity remains in the determination of the b-plane orientation of the field at high temperature. A combined noncoaxial magnetic and electric interaction was explicitly taken into account in the theoretical analysis of the experimental spin precession curves. The interpretation of the obtained magnetic anisotropy results included terms up to the third order in the energy-density function to explain the b-plane orientation of the field.

II. EXPERIMENTAL TECHNIQUE

A cobalt single crystal was prepared as a 12.5-mm diameter disc with 0.4 mm thickness. The c axis was in the plane of the disc, and the $\langle 10\bar{1}0\rangle$ axis was perpendicular to the disc plane. The crystal was implanted at room temperature with ^{111}In to a dose of 5×10^{13} ions/cm^2, with an implantation energy of 80 keV. The mean value of the range profile is 16 nm with $\Delta R_p=6$ nm. The indium radioactivity decays with a 2.81 d half-life to ^{111}Cd, used as probe in the PAC experiment. This is a particularly convenient probe because its hyperfine field is different in hcp and fcc phases, which can coexist at room temperature.[19] No fcc phase was found to exist in the crystal.

The time-differential perturbed-angular correlation of the 175 and 247 keV γ transitions of the cascade in ^{111}Cd was measured with a time resolution of 0.6 ns using four BaF_2 detectors. All detectors were in the same plane, making 90° angles with each other such that four correlation spectra $W(\mathbf{k}_1,\mathbf{k}_2,t)$ were obtained. $W(\mathbf{k}_1,\mathbf{k}_2,t)$ is the time-dependent directional correlation function between two γ radiations emitted in the directions $\mathbf{k}_1\equiv(\theta_1,\phi_1)$ and $\mathbf{k}_2\equiv(\theta_2,\phi_2)$. Apart from the well-known nuclear parameters, this function also depends on the hyperfine interaction, i.e., strength and orientation of the magnetic hyperfine field and electric-field gradient (EFG), and can be written as

$$W(\mathbf{k}_1,\mathbf{k}_2t)=\sum_{\lambda\lambda'\mu\mu'}(-1)^{\lambda'}A_{\lambda\lambda'}[(2\lambda+1)(2\lambda'+1)]^{-1/2}\times G_{\lambda\lambda'}^{\mu\mu'}(t)Y_\lambda^{\mu*}(\theta_1,\phi_1)Y_{\lambda'}^{\mu'}(\theta_2,\phi_2)\ , \quad (1)$$

with

$$G_{\lambda\lambda'}^{\mu\mu'}(t)=\sum_{\mu\bar{m}mnn'}(-1)^{2I+m+m'}[(2\lambda+1)(2\lambda'+1)]^{1/2}\times\exp(-i\omega_{nn'}t)u_{nm}u_{nm'}^{*}u_{n'\bar{m}}^{*}u_{n'\bar{m}'}\times\begin{bmatrix}I & I & \lambda\\ \bar{m} & -\bar{m}' & \mu\end{bmatrix}\begin{bmatrix}I & I & \lambda'\\ m & -m' & \mu'\end{bmatrix}\ . \quad (2)$$

$A_{\lambda\lambda'}$ determines the amplitude of the signal, the spherical harmonics $Y_\lambda^\mu(\theta,\phi)$ define the geometry of detection. All the information about the interaction is on the perturbation factor $G_{\lambda\lambda'}^{\mu\mu'}(t)$. I is the spin of the probe in the intermediate state of the cascade ($\frac{5}{2}$ for ^{111}Cd); n, n', m, m', $\bar{m}$, and $\bar{m}'$ correspond to different sublevels of that state [$\bar{m}$ and $\bar{m}'$ are defined through the circular relations of the $3-j$ symbols $\bar{m}+(-m)+\mu=0$ and $\bar{m}'+(-m')+\mu=0$]; λ, λ', μ, and μ' are summation indexes that depend on the cascade. The frequencies $\omega_{nn'}=\omega_n-\omega_{n'}$ correspond to the transitions between different sublevels, where ω_n and u_{nm} are the eigenvalues and eigenvectors of the interaction Hamiltonian. Its general form, written in the EFG system,[20] results in the matrix elements,

$$\begin{aligned}H_{m,m}^{\mathrm{el}}&=\hbar\omega_Q[3m^2-I(I+1)]\\ H_{m,m\pm2}^{\mathrm{el}}&=\hbar\omega_Q\eta[(I\mp m-1)(I\mp m)(I\pm m+1)\times(I\pm m+2)]^{1/2}/2\\ H_{m,m}^{\mathrm{mag}}&=\hbar\omega_L\cos\beta m\\ H_{m,m\pm1}^{\mathrm{mag}}&=\hbar\omega_L[I(I+1)-m(m\pm1)]^{1/2}\sin\beta e^{\pm i\gamma}/2\ .\end{aligned} \quad (3)$$

This Hamiltonian is equivalent to the one presented in Ref. 21, where it is written in the magnetic-field system. The EFG system was chosen because it is preferable, for computational reasons, to work with a fixed quantization axis, and in cobalt the EFG is expected to have always the c-axis orientation,[18] while the magnetization direction is expected to change with temperature.[1–3] The magnetic-field system is normally used in situations where the magnetic field has a fixed direction, as in Ref. 21 for applied magnetic field and random EFG.

For a magnetic or an axially symmetric ($\eta=0$) electric interaction, $W(\mathbf{k}_1,\mathbf{k}_2,t)$ is a periodic function with frequency equal, respectively, to the magnetic Larmor ω_L or electric ω_0 interaction frequencies

$$\omega_L=-\frac{\mu B_{\mathrm{hf}}}{I\hbar}$$

or

$$\begin{aligned}\omega_0&=3\frac{eQV_{zz}}{4I(2I-1)\hbar}=3\omega_Q,\quad \text{for } I \text{ integral}\ ,\\ \omega_0&=6\frac{eQV_{zz}}{4I(2I-1)\hbar}=6\omega_Q,\quad \text{for } I \text{ half integral}\ .\end{aligned} \quad (4)$$

Harmonics can also be observed, depending on the orientation of the fields. For $\eta>0$, the relation between ω_0 and ω_Q depends on the value of η. For a combined magnetic and electric interaction, ω_{mn} are the observable frequencies. B_{hf} is the magnetic hyperfine field, V_{zz} is the main component of the electric-field-gradient tensor, $\eta=(V_{xx}-V_{yy})/V_{zz}$ is the asymmetry parameter, β and γ are Euler angles defining the orientation of the magnetic field relative to the EFG, β being the angle between the magnetic field and the principal z axis of the EFG (c axis for a hcp structure). Notice that the angles defined as β and γ in Ref. 21 define the EFG relative to the magnetic-field system, and hence are not equal to the ones used here, taken from Ref. 20; however, in both cases β is the angle between V_{zz} and B_{hf}, although it is defined with opposite signs.

In order to eliminate the nuclear decay function and to minimize effects due to different detector efficiencies, the anisotropy factor or spin precession function $R(t)$ is used:

$$R(t)=2\frac{N(180°,t)-N(90°,t)}{N(180°,t)+2N(90°,t)}\ , \quad (5)$$

with θ the angle between the radiation directions $\mathbf{k}_1$ and $\mathbf{k}_2$, and

$$N(\theta,t)=\left[\prod_{j=1}^{N_\theta}W_j(\theta,t)\right]^{1/N_\theta}\ . \quad (6)$$

N_θ is the number of spectra taken at angle θ.

III. NUMERICAL CALCULATIONS

The correlation function $W(\mathbf{k}_1\mathbf{k}_2t)$ was calculated numerically taking into account the full Hamiltonian, the geometry of detection, and the $G_{\lambda\lambda'}$ terms up to $\lambda,\lambda'=4$, including the cross terms (for the cascade of ^{111}Cd used, A_{24} is larger than A_{22}, even after solid angle corrections). Then a theoretical $R(t)$ spin precession function was calculated, using exactly the same formal expression as the experimental one, with no approximations and incorporated in a least-squares fitting routine, where all the parameters are physically meaningful.

Calculated spectra for $I=\frac{5}{2}$ are shown in Fig. 1 for a collinear interaction with $\omega_L/\omega_0=70$ and $\eta=0$ (corresponding to the actual values in cobalt at room temperature[18]) for a polycrystalline sample, and for a single crys-

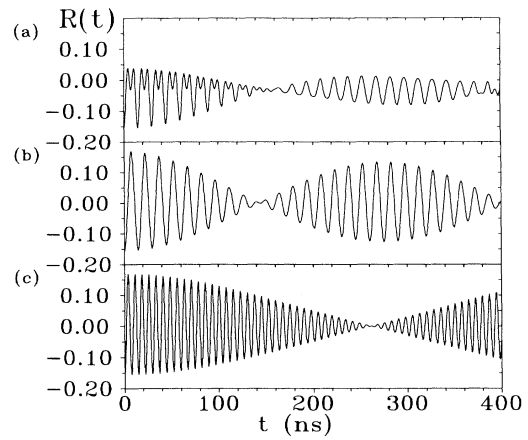

FIG. 1. Theoretical spectra calculated for a combined coaxial interaction with $\omega_L/\omega_0=70$ and $\eta=0$, for (a) polycrystal; (b) single crystal with fields in the detectors' plane; (c) single crystal with fields perpendicular to the detectors' plane. While for polycrystals the "ω_L and $2\omega_L$ frequencies" are always observed, in single crystals it depends on the fields' orientation.

tal in two different orientations of the c axis: the first with the c axis in the plane of the detectors (d plane) at a 45° angle with them, and the second with the c axis perpendicular to that plane. Notice that η cannot be determined for such a large value of y. Lindgren, Bedi, and Wappling[18] assumed it to be zero due to the sixfold rotational symmetry of cobalt's hcp lattice, and the same assumption is done in this work. It does not affect the determination of the magnetic-field value and direction.

In the three spectra a beating pattern is observed, as is expected for a dominant magnetic interaction.[22] These spectra can be seen in perturbation theory[23] as a pure magnetic oscillation enfolded by the electric oscillation. In fact, the observed frequencies are, for collinear interaction, $\omega_L\pm\omega_0,\omega_L\pm2\omega_0$, in the present context referred to as "ω_L frequencies," and $2\omega_L\pm\omega_0,2\omega_L\pm3\omega_0$, referred to as "$2\omega_L$ frequencies." For noncollinear interactions, the electric splitting of the "ω_L and $2\omega_L$ frequencies" is reduced, depending on the angle β.

While in a polycrystal the "ω_L frequencies" and "$2\omega_L$ frequencies" are always observed with equal amplitudes, in a single crystal their amplitudes depend on the orientation of the magnetic field. Only the "ω_L frequencies" are observed if the magnetic field lies in the detector plane at a 45° angle with the detectors, while only the "$2\omega_L$ frequencies" are observed when perpendicular to that plane. No other four-detector setup geometries can produce those results. In a three-detector setup, one uses one start and two stop detectors at 90° and 180° angles with the start detector. If the field is oriented along the stop detector (thus at 90° with the start) only the "$2\omega_L$ frequencies" are observed. If the field makes a small angle with the start detector, then preferentially the "ω_L frequencies" are observed, but with reduced amplitude. The fact that the change of the magnetic-field direction induces a dramatic change in the relative amplitudes of the "ω_L and $2\omega_L$ frequencies," allows an accurate determination of that direction.

IV. RESULTS

Experiments were done between room temperature and 663 K. The temperature stability was within 1 K. The c axis was set perpendicular to the detector plane, with the $\langle 10\bar{1}0\rangle$ axis in that plane at 45° with the detectors. This crystal orientation was chosen to assure that at room temperature the magnetic hyperfine field would be perpendicular to the detector plane, but in the plane at high temperature. The results obtained between 493 and 613 K are shown in Fig. 2. The transition from the "$2\omega_L$ to the ω_L frequencies" is clearly seen, reflecting the changing of the magnetization direction from the c axis to the basal plane. The β angle in the intermediate temperatures can be derived with an accuracy of about 3°.

Remarkably, only the "ω_L frequencies" are seen at 613 K and above, indicating that the magnetic field is in the plane and at 45° with the detectors, but in a single well-defined direction and not a threefold one as expected from the hexagonal symmetry. From the positioning of the crystal, that direction is either the $\langle 10\bar{1}0\rangle$ or the $\langle 1\bar{2}10\rangle$ axis. To discriminate between these two possibilities, a new experiment was done, with the c axis in the same position, but with the $\langle 10\bar{1}0\rangle$ axis making a 10° angle with one of the start detectors and 80° with the other. Calculating two independent three-detector $R(t)$ functions, one for each start detector, instead of the usual four-detector function, we obtained physically different functions. Their Fourier transforms are shown in Fig. 3, where the two start detectors were named A and B. The

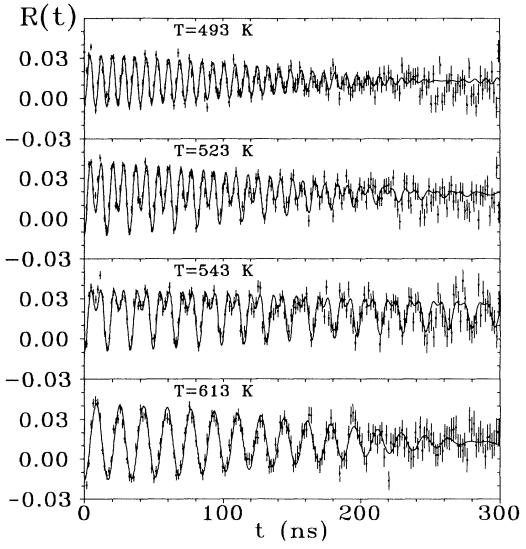

FIG. 2. Spectra taken between 493 and 613 K, with the c axis perpendicular to the detectors' plane. The transition from the "$2\omega_L$ to the ω_L frequencies" indicates the transition of the magnetization from the c axis to the basal plane. At 613 K only the "ω_L frequencies" are seen, which shows that the magnetization is in one single direction (see text).

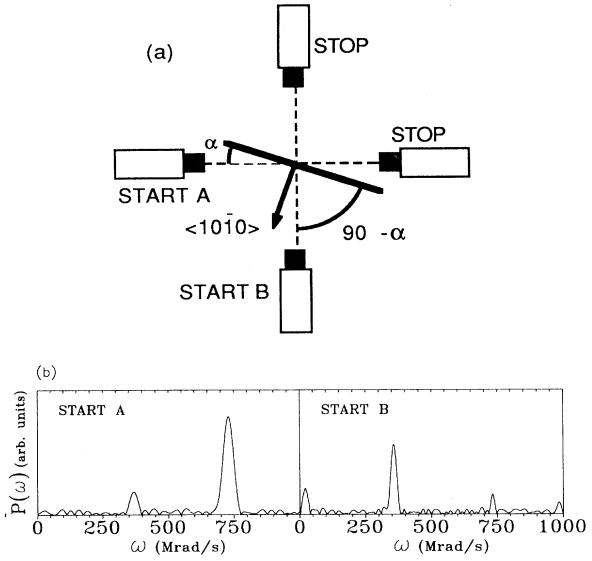

FIG. 3. (a) Geometry used to determine the basal-plane orientation of the magnetization. Three-detector spectra were built, one for each start detector. (b) Fourier transforms of the two three-detector spectra obtained, allowing to conclude that the magnetization was near start B, therefore along the $\langle 10\bar{1}0\rangle$ axis.

differences seen correspond to a magnetic field near detector B, so we conclude that in this crystal the magnetic hyperfine field is along the $\langle 10\bar{1}0\rangle$ axis above 613 K.

V. DISCUSSION

A. Temperature dependence of B_{hf}, V_{zz}, and β

The room-temperature value of the hyperfine field is $B_{hf}=288(3)$ kG, where the error in the ^{111}Cd g factor $g=0.306(1)$ (Ref. 24) was included. The measured temperature dependence of B_{hf} is shown in Fig. 4 together with the magnetization of bulk cobalt. It reproduces the results of Lindgren, Bedi, and Wappling.[18]

If a polycrystalline sample is used the simultaneous determination of β and ω_0 is in general not possible for a dominant magnetic interaction, because different combinations of values of β and ω_0 produce very similar spectra. The use of single crystals allows more than one geometry of detection and then both parameters can easily be determined. At room temperature, we analyzed two different geometries and obtained $\beta=0°$, as expected, with $\omega_0=6.03(13)$ Mrad/s yielding $V_{zz}=32(5)\times10^{15}$ V/cm^2, taking into account the error in the quadrupole moment $Q=0.83(13)$ b.[25] These results are in agreement with values obtained previously,[18,26,27] but here with a much smaller error (the errors we quote include a 1% calibration error). At high temperature we used only one geometry, obtaining $\omega_0=5.9(3)$ Mrad/s, but we had to assume $\beta=90°$ at 663 K, which should not be a problem since the magnetic field is seen to be in the basal plane already at 613 K. As there is no variation, within

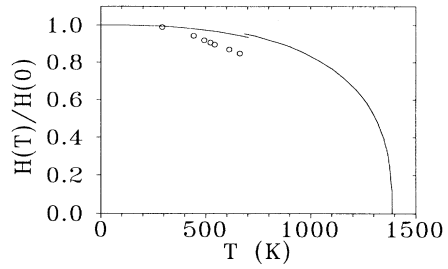

FIG. 4. Temperature dependence of the reduced hyperfine field vs reduced magnetization. The results reproduce those of Ref. 18.

the experimental error, of ω_0 with temperature, we kept it fixed at its room-temperature value to obtain β in the intermediate temperatures range. Notice that, since it's the magnetic field that rotates, choosing the quantization axis along the fixed V_{zz}, and therefore writing the Hamiltonian in the EFG system, makes the calculations much easier. The temperature dependence of β is given in Fig. 5, together with the dependence derived from the values of the anisotropy constants K_1 and K_2, obtained by Ono[2] at a constant applied field of 16.9 kOe. Both results agree very well, thereby confirming that the field-dependent term in the anisotropy of cobalt is small. Ono showed that this variation comes mainly from the thermal expansion of cobalt's hcp lattice, and is not related to the transition to the fcc phase that occurs around 700 K.

B. Basal-plane anisotropy

The anisotropy energy density for a hexagonal system is written, including terms up to the third order, as

$$E_k=K_1\sin^2\beta+K_2\sin^4\beta+K_3\sin^6\beta+K_4\sin^6\beta\cos 6\phi\ , \quad (7)$$

where β is the angle between the magnetization and the c axis, and ϕ is the angle between its projection on the basal plane and one b axis. The minimization of E_k in respect to β can be done ignoring the terms in K_3 and K_4, and provides the temperature dependence of β as function of K_1 and K_2, used in Fig. 5. Its minimization in respect to ϕ provides the basal-plane orientation of the magnetiza-

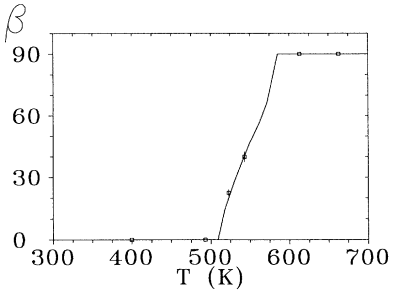

FIG. 5. Temperature dependence of β as derived from the present experimental data vs β as derived from the magnetocrystalline anisotropy constants K_1 and K_2 taken from Ref. 2 (continuous line). The error in the determination of β with this method is of the order of 10°.

tion. Paige, Szpunar, and Tanner[1] measured K_4 between 70 and 415 K, where it decreases from 12×10^4 erg/cm^3 to 1×10^4 erg/cm^3, a factor of 100 smaller than K_1 at room temperature. From these results the magnetization would be in three equivalent directions, being $\langle 10\bar{1}0\rangle$, $\langle \bar{1}100\rangle$, and $\langle 01\bar{1}0\rangle$, at 30° with the b axes. However, in the single crystal we used, we found only one preferential orientation of the magnetization in the basal plane, the $\langle 10\bar{1}0\rangle$ axis. This can be explained only if an additional uniaxial term is introduced in the anisotropy energy density,

$$E_{k,\text{tot}}=E_k+E_u, \quad \text{with } E_u=K_u\sin^2(\phi-\pi/6)\ . \tag{8}$$

The minimization of $E_{k,\text{tot}}$ yields in general six solutions, depending on the K_u/K_4 ratio. The $\langle 10\bar{1}0\rangle$ axis is the simple solution (in fact it consists of the two solutions $\phi=\pi/6$ and $\phi=\pi+\pi/6$) only if

$$\begin{aligned} &K_u\geq 6K_4\geq 0, \quad \text{for positive } K_4\ , \\ &K_u\geq -18K_4\geq 0 \quad \text{for negative } K_4\ , \end{aligned} \tag{9}$$

therefore a value for K_u of the order of 10^5 erg/cm^3 is necessary to explain the observed uniaxial anisotropy.

C. Origin of the basal-plane anisotropy

This uniaxial anisotropy induces a breaking of the lattice symmetry in the basal plane, likely due to the fact that the $\langle 10\bar{1}0\rangle$ axis is perpendicular to the surface of our crystal. Recently, perpendicular anisotropy has been discovered in very thin ferromagnetic films,[28] and explained in terms of a surface anisotropy term E_s arising from the breaking of the (magnetic) symmetry for the atoms at the surface. The corresponding anisotropy constant is

$$K_{us}=2K_s/t\ , \tag{10}$$

with t the thickness of the film. This term, inversely proportional to t, is very small for a thick sample. For the Au-Co interface $K_s\approx 0.5$ erg/cm^2,[29] which gives for our crystal $K_{us}\approx 10$ erg/cm^3, much too small to explain our results.

An alternative explanation is that a unidirectional deformation of the lattice normal to the crystal (arising possibly during the growth of the flat crystal used) could induce the additional magnetic anisotropy, as opposite to magnetostriction, where a change in magnetization is accompanied by a change of length. This is known in iron, where the effect of stress is to create a preferred direction of magnetization along the stress direction.[19] Evidence of such uniaxial volume stress-induced anisotropy was also found in cobalt thin films.[28] The change of length in cobalt in a direction cosines β_1,β_2,β_3, coming from a change of magnetization from zero to saturation in a direction cosines $\alpha_1,\alpha_2,\alpha_3$, is

$$\begin{aligned} dl/l=&\lambda_A(\alpha_1\beta_1+\alpha_2\beta_2)(\alpha_1\beta_1+\alpha_2\beta_2-\alpha_3\beta_3) \\ &+\lambda_B[(1-\alpha_3^2)(1-\beta_3^2)-(\alpha_1\beta_1+\alpha_2\beta_2)^2] \\ &+\lambda_C[(1-\alpha_3^2)\beta_3^2-(\alpha_1\beta_1+\alpha_2\beta_2)\alpha_3\beta_3] \\ &+4\lambda_D(\alpha_1\beta_1+\alpha_2\beta_2)\alpha_3\beta_3\ , \end{aligned} \tag{11}$$

in an orthogonal system, with $\lambda_A=-45\times10^{-6}$, $\lambda_B=-95\times10^{-6}$, $\lambda_C=+110\times10^{-6}$, and $\lambda_D=-100\times10^{6}$.[30] Assuming that an inverse relation is valid between a deformation of the crystal and the resulting magnetization m and that the relation is linear on the intensity of the magnetization, then for a deformation along the crystal normal we obtain

$$m=\frac{dl/l}{\lambda_A}M\ , \tag{12}$$

where M is the saturation magnetization of cobalt. The resulting deformation anisotropy constant can be calculated as $K_{ud}=(4\pi m^2)/2$, as seen above of the order of 10^5 erg/cm^3. From these formulas we derive $dl/l\approx 3\times10^{-7}$ for the lattice deformation needed to cause the observed uniaxial anisotropy. This value has only qualitative meaning in view of the assumptions made, namely taking for λ_A the value obtained for magnetostriction.

VI. CONCLUSIONS

We used the perturbed-angular-correlation technique to study the temperature dependence of the hyperfine magnetic field and electric-field gradient of cadmium in cobalt and of the magnetocrystalline anisotropy of cobalt single crystal without use of an applied field. The results obtained for the angle β between the magnetization and the c axis agree very well with the uniaxial anisotropy constants K_1 and K_2 obtained by torque magnetometry. Instead of the expected threefold axial symmetry the existence of a single preferred orientation of the magnetization in the basal plane was found and explained in terms of deformation-induced anisotropy, normal to the c-plane crystal surface. A threefold symmetry has been found previously[1] in a basal-plane cut crystal, where normal stress would have no influence.

We stress that the use of single crystals allowed us to observe the preferential basal-plane anisotropy and to obtain a higher precision on the values for the hyperfine fields when compared to the ones obtained using polycrystalline samples.

ACKNOWLEDGMENTS

One of us (N.P.B.) acknowledges the Junta Nacional de Investigação Científica e Tecnológica (Programa Ciência) and the Erasmus for financial support.

[1]D. Paige, B. Szpunar, and B. Tanner, J. Magn. Magn. Mater. **44**, 239 (1984).
[2]F. Ono, J. Phys. Soc. Jpn. **50**, 2564 (1981).
[3]W. Sucksmith and J. Thompson, Proc. R. Soc. London A **225**, 362 (1954).
[4]A. Jain and T. Cranshaw, Phys. Lett. **25A**, 421 (1967).
[5]T. Cranshaw, J. Appl. Phys. **40**, 1481 (1969).
[6]G. Huffman and G. Dunmyre, J. Appl. Phys. **41**, 1323 (1970).

[7]M. Kwakami, T. Hihara, Y. Koi, and T. Wakiyama, J. Phys. Soc. Jpn. **33**, 1591 (1972).
[8]M. Kwakami and Y. Koi, J. Phys. Soc. Jpn. **37**, 1257 (1974).
[9]P. Raghavan, M. Senba, and R. Raghavan, Phys. Rev. Lett. **39**, 1547 (1977).
[10]N. Nishida, K. Nagamine, R. Hayano, T. Yamazaki, D. Fleming, R. Duncan, J. Brewer, A. Akhtar, and H. Yasuoka, Hyperfine Interact. **4**, 318 (1978).
[11]R. Reno, Hyperfine Interact. **4**, 338 (1978).
[12]G. Wortmann, B. Perscheid, G. Kaindl, and F. Wagner, Hyperfine Interact. **4**, 343 (1978).
[13]B. Lindgren and Y. Vijay, Hyperfine Interact. **4**, 379 (1978).
[14]K. Johansson, W. Karner, B. Lindgren, L. Norlin, and G. Possnert, Hyperfine Interact. **9**, 409 (1981).
[15]M. Senba, P. Raghavan, W. Semmler, and R. Raghavan, Hyperfine Interact. **9**, 449 (1981).
[16]M. Senba, P. Raghavan, W. Semmler, and R. Raghavan, Hyperfine Interact. **9**, 453 (1981).
[17]A. Kleinhammes and C. Hohenemser, Hyperfine Interact. **59**, 403 (1990).
[18]B. Lindgren, S. Bedi, and R. Wappling, Phys. Scr. **18**, 26 (1978).
[19]R. Tebble and D. Craik, *Magnetic Materials* (Wiley, New York, 1969), pp. 28 and 68-73.
[20]L. Bostrom, E. Karlsson, and S. Zeterlund, Phys. Scr. **2**, 65 (1970).
[21]E. Matthias, W. Schneider, and R. M. Steffen, Ark. Fys. **24**, 97 (1962).
[22]H. Haas, Phys. Scr. **11**, 221 (1975).
[23]E. Dafni and G. Sprouse, Hyperfine Interact. **4**, 777 (1978).
[24]H. Bertschat, H. Haas, F. Pleiter, E. Recknagel, E. Schlodder, and B. Spellmeiyer, Z. Phys. A **270**, 203 (1974).
[25]R. Vianden, Hyperfine Interact. **35**, 1079 (1987).
[26]F. Raether, D. Wiarda, K. P. Lieb, J. Chevallier, and G. Weyer, Z. Phys. B **73**, 467 (1989).
[27]G. McGhee and G. Collins, Hyperfine Interact. **60**, 659 (1990).
[28]C. Chappert, K. Dang, P. Beauville, H. Hurdequint, and D. Renard, Phys. Rev. B **34**, 3192 (1986).
[29]C. Chappert and P. Bruno, J. Appl. Phys. **64**, 5736 (1988).
[30]R. Bozorth, Phys. Rev. **96**, 311 (1954).